Interference fringes of the atom interferometer comprised of four copropagating traveling laser beams

Shinya Yanagimachi, Yasuo Omi, and Atsuo Morinaga
Department of Physics, Faculty of Science and Technology, Science University of Tokyo, 2641 Yamazaki, Noda-shi, Chiba 278, Japan
(Received 22 September 1997)

An atom interferometer comprised of four copropagating traveling laser beams has been developed using a thermal calcium atomic beam and the performance of the interference fringes was investigated experimentally. The interference fringes with a visibility of 0.2 were observed at an excitation power of 0.6 mW. The signal-to-noise ratio was about 100 at an integration time of 5 ms. The equations for the interference signal were derived from the evolution matrices of spinors and the visibility was calculated in consideration of the divergent thermal atomic beam. The experimental results were described well by the present calculation. [S1050-2947(98)02605-5]

PACS number(s): 03.75.Dg, 42.50.Vk

I. INTRODUCTION

Atomic interferometers are expected to be used as sensitive detectors in a variety of precision measurements, since the de Broglie wavelengths of atoms are about 10 000 times shorter than those of light. Moreover, atomic interferometers have the potential for applications in new experiments where neutron or electron interferometry is not applicable, using the atom's internal energy structure. Since 1991, several versions of the atomic interferometer have been presented [1–5].

A typical atom interferometer using coherent deflection of an atomic beam by light is the Ramsey-Bordé atom interferometer [6]. A thermal atomic beam interacts with four laser beams, two of which propagate in one direction and the others in the opposite direction, and forms a trapezoidal trajectory. The phase difference between two trajectories is given by the detuning frequency, optical phase difference, and atomic phase shift caused by external perturbations. Therefore in this interferometer phase shift can be measured precisely from frequency shift of the resonance frequency. The Sagnac effect [3], ac and dc Stark effect [7–9], and recently the Aharonov-Casher effect [10] were measured by this interferometer. However, this interferometer requires a highly frequency-stable laser to measure an extremely small phase shift.

On the other hand, four laser beams traveling in the same direction form a closed trajectory in the shape of a parallelogram. In this case, the phase shift is determined by only the differences between optical phase and atomic phase, since the two trajectories are symmetric. This means that this interferometer is far less sensitive to frequency fluctuations of the laser. And this interferometer works like a white light interferometer, so that it may be suited to measure the phase of the Aharonov-Casher effect which is independent of atomic wavelength.

Such an atomic interferometer was discussed by Bordé a few years ago [11]. Previously a very similar interferometer geometry has been realized using a $\pi/2$-π-$\pi/2$ pulse sequence with Raman transitions by Kasevich and Chu [4,12]. In their case, laser pulses separated in time were used for cold atoms. On the other hand, Morinaga and Ohuchi have developed this interferometer using a thermal calcium atomic beam [13] and have already derived an equation for the interference signal of the interferometer composed of four traveling laser beams and calculated the interference signal for a phase shift due to dc Stark effect [14]. The behavior of the experimental results was reproduced by the calculation, however, the divergence of the thermal atomic beam was not taken into account. Therefore we derive an equation of the interference fringes for a divergent thermal atomic beam. The resonance profile is calculated as a function of the detuning of laser frequency and the visibility of the interference fringes is obtained.

This paper describes the performance of the calcium atomic interferometer comprised of four copropagating trav-

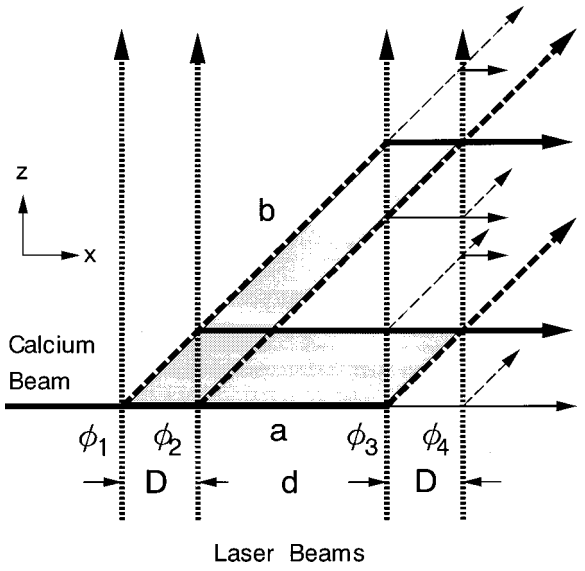

FIG. 1. Interaction geometry of the atom interferometer with four copropagating traveling laser beams. Two pairs of trajectories make two interferometers. a, ground state (solid line); b, excited state (broken line); ϕ_i, phase of the ith laser beam (dotted line) at time t; and D and d are beam intervals.

eling laser beams which was investigated experimentally. The experimental results are compared with the calculation which is derived in this paper.

II. PRINCIPLE

We consider a two-level atom interacting with four traveling laser beams which propagate in the z direction. The laser beams have the same frequency ω_0 and the same power p. The geometrical paths of the atom are shown in Fig. 1. The atomic waves which move in the x direction interact with the laser beams and split into two paths: the path of the excited state b, which has a recoil velocity in the z direction in addition to the initial velocity, and the path of the ground state with an initial velocity a. After the atom interacts with the four laser beams, there are 16 trajectories. When the beam spacing between the first and the second interactions is equal to that between the third and the fourth ones, two Mach-Zehnder interferometers are formed by two pairs of trajectories, as seen in Fig. 1. The interference fringes are obtained from the variation of the population probability of either the upper state or the lower state. Conventionally, we observe the population probability of the excited atom by monitoring the fluorescence signal from the excited state. Therefore, in the present paper, we consider eight trajectories whose final states are the excited state in order to calculate the interference fringes.

The wave function of the atom in the excited state b after interactions with four copropagating laser beams is described using the method of the evolution matrices of spinors derived by Bordé *et al.* [15].

$$
\begin{aligned}
b = \exp(-\gamma_b\tau)\exp\{i(-\delta-kv_z)(T'+2T+4\tau)/2\}[&B_1A_2A_3A_4\ \exp\{-\gamma_b(2T+T')/2\}\exp\ i\{(\Delta-kv_z-\delta)(2T+T')/2-\phi_1\}\\
&+D_1B_2A_3A_4\ \exp\{-\gamma_b(T+T')/2\}\exp\ i\{(\Delta-kv_z-\delta)2T'/2-\phi_2\}\\
&+B_1A_2C_3B_4\ \exp\{-\gamma_b(T+T')/2\}\exp\ i\{(\Delta-kv_z-\delta)2T'/2-\phi_1+\phi_3-\phi_4\}\\
&+D_1B_2C_3B_4\ \exp(-\gamma_bT'/2)\exp\ i\{-(\Delta-kv_z-\delta)(2T-T')/2-\phi_2+\phi_3-\phi_4\}\\
&+B_1C_2B_3A_4\ \exp(-\gamma_bT)\exp\ i\{(\Delta-kv_z-\delta)(2T-T')/2-\phi_1+\phi_2-\phi_3\}\\
&+D_1D_2B_3A_4\exp(-\gamma_bT/2)\exp\ i\{-(\Delta-kv_z-\delta)T'/2-\phi_3\}\\
&+B_1C_2D_3B_4\ \exp(-\gamma_bT/2)\exp\ i\{-(\Delta-kv_z-\delta)T'/2-\phi_1+\phi_2-\phi_4\}\\
&+D_1D_2D_3B_4\exp\ i\{-(\Delta-kv_z-\delta)(2T+T')/2-\phi_4\}].
\end{aligned}
\tag{1}
$$

Notations used here are the same as those used by Bordé *et al.* [15]: Δ is the detuning frequency from ω_0, δ is photon recoil, k is wave number of light, v_x and v_z are initial velocities of the atom in the x and z directions, γ_b is the relaxation constant of the excited state, and ϕ_i is the optical phase. Subscript i denotes the number of interaction zones. T, T', and τ are pass times of the first (or third) and central field-free zone and laser beam, respectively. There are D/v_x, d/v_x, and $2w/v_x$, where D and d are lengths of the first and central field-free zone and w is a radius of the laser beam. A_i, B_i, C_i, and D_i are parameters which describe the transition between states. Each of the eight terms corresponds to one of the eight trajectories in sequence, as shown in Fig. 1.

The population probability of the excited state can be obtained from the product of b with its complex conjugate,

$$
\begin{aligned}
bb^* = \exp(-2\gamma_b\tau)[&|B_1A_2A_3A_4|^2\ \exp\{-\gamma_b(2T+T')\}+|D_1B_2A_3A_4|^2\ \exp\{-\gamma_b(T+T')\}\\
&+|B_1A_2C_3B_4|^2\exp\{-\gamma_b(T+T')\}+|D_1B_2C_3B_4|^2\ \exp(-\gamma_bT')+|B_1C_2B_3A_4|^2\ \exp(-2\gamma_bT)\\
&+|D_1D_2B_3A_4|^2\exp(-\gamma_bT)+|B_1C_2D_3B_4|^2\exp(-\gamma_bT)+|D_1D_2D_3B_4|^2\\
&+\{(B_1A_2C_3B_4)(D_1B_2A_3A_4)^*\ \exp\{-\gamma_b(T+T')\}\exp\ i\Delta\phi+\text{c.c.}\}\\
&+\{(B_1C_2D_3B_4)(D_1D_2B_3A_4)^*\exp(-\gamma_bT)\exp\ i\Delta\phi+\text{c.c.}\}+O(\exp(\pm ikv_zT),\exp(\pm 2ikv_zT))],
\end{aligned}
\tag{2}
$$

where $\Delta\phi$ denotes the optical phase difference, namely, $\Delta\phi=-\phi_1+\phi_2+\phi_3-\phi_4$. The first eight terms are noninterference terms and give the background population. The next two terms having the optical phase give the interference fringes and correspond to the two interferometers in the figure. Since the four laser beams have the same power, the phases of the two interferometers become the same. The other terms proportional to a function of exponential of kv_zT or $2kv_zT$ vanish by the integrals of v_z on the assumption that the residual Doppler width is large compared to the fringe width. Therefore we omit them from the equation in the calculation hereafter.

When an atom with a particular velocity of v_x interacts at a right angle with laser beams of a resonance frequency, the population probability of the excited state is calculated by the following equation:

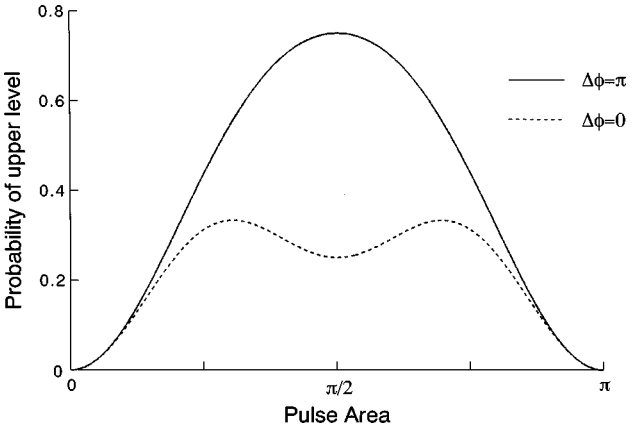

FIG. 2. Probability of the excited state for the phase difference of π rad (solid line) and 0 rad (dotted line), as a function of pulse area.

$$
\begin{aligned}
bb^*(v_x,\theta) = \exp(-2\gamma_b\tau)\sin^2\frac{\theta}{2}\cos^2\frac{\theta}{2}
&\times\left(\left\{1+\exp\left(-\gamma_b\frac{D}{v_x}\right)+\exp\left[-\gamma_b\left(\frac{D+d}{v_x}\right)\right]\right.\right.\\
&\left.+\exp\left[-\gamma_b\left(\frac{2D+d}{v_x}\right)\right]\right\}\cos^4\frac{\theta}{2}\\
&+\left\{\exp\left(-\gamma_b\frac{D}{v_x}\right)+\exp\left(-2\gamma_b\frac{D}{v_x}\right)\right.\\
&\left.+\exp\left(-\gamma_b\frac{d}{v_x}\right)+\exp\left(-\gamma_b\frac{D+d}{v_x}\right)\right\}\\
&\times\sin^4\frac{\theta}{2}-2\left\{\exp\left(-\gamma_b\frac{D}{v_x}\right)\right.\\
&\left.\left.+\exp\left(-\gamma_b\frac{D+d}{v_x}\right)\right\}\sin^2\frac{\theta}{2}\cos^2\frac{\theta}{2}\cos\Delta\phi\right),
\end{aligned}
\tag{3}
$$

where $\theta=\Omega_{ab}\tau$ is the pulse area and Ω_{ab} is the Rabi frequency. The results are shown in Fig. 2, as a function of various pulse areas. The solid line is the population probability for optical phase of π rad, and the dashed line is that for 0 rad. When the pulse area is $\pi/2$, the probability of the excited state is changed from 0.75 to 0.25 depending on the optical phase difference. Therefore the maximum visibility of 0.5 can be obtained at the excitation of $\pi/2$ pulse using the present atom interferometer.

III. EXPERIMENT

The experimental setup is shown in Fig. 3. A thermal calcium atomic beam with the most probable velocity of 780 m/s, which corresponds to de Brogie wavelength of 13 pm, was generated from an oven at a temperature of 700 °C. It is collimated to give a residual Doppler full width of about 3 MHz using two diaphragms. An output beam with a wavelength of 657 nm and a frequency stability of 20 kHz from a high-resolution dye laser spectrometer [16] was used to excite calcium atoms to the $^3P_1$ state from the ground state

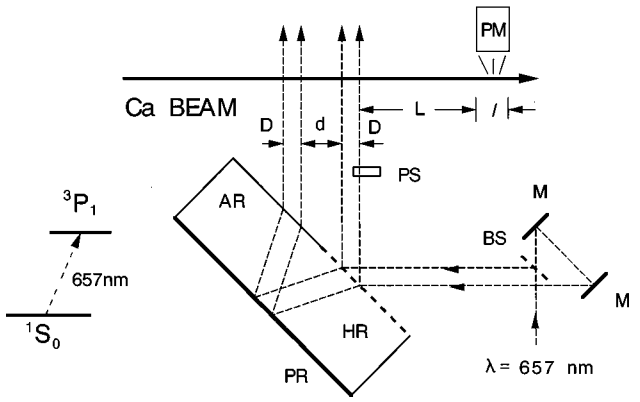

FIG. 3. Experimental setup for the calcium atom interferometer, together with a partial energy diagram of Ca. PS, phase shifter; PM, photomultiplier; BS, beam splitter; M, mirror; AR, antireflection; HR, half reflection; and PR, perfect reflection.

$^1S_0$. The laser beam is transferred to the atomic beam apparatus by a polarization-preserving optical single-mode fiber. The laser beam was collimated by a high-quality microscope lens so as to be a beam waist at the zone where it interacts with the atomic beam. The radius of the beam waist is 1.55 mm. The output intensity was stabilized at the exit of the fiber to be less than 0.1% at an integration time of 5 ms.

In order to generate two parallel laser beams with equal power, we used an optical parallel plate. One-half of the front surface of this plate reflects 50% of the beam and the other is coated with an antireflection coating. The rear surface has a perfect reflection coating. The beam space between two beams is 20 mm and the parallelism is within 1 s. We introduce two parallel beams with equal power into this optical plate. The beam interval D between the two incident beams is changed from 5 to 15 mm. The parallelism of the two incident beams is tested by monitoring the spectrum, so that both laser beams interact with the same atoms within a resonance width of about hundreds of kilohertz. A small magnetic field was applied perpendicular to both the atomic beam and the laser beams in the interaction zone. The polarization of the laser beam was set so as to excite only the $\Delta m=0$ transition. The fluorescence from the $^3P_1$ state with a lifetime of 0.4 ms is detected at $L=250$ mm downstream by a photomultiplier with a diameter of $l=5$ cm. A glass plate was mounted on a scanning galvanometer and it was inserted in the path of the fourth beam before interaction with the atomic beam and was tilted in order to give atoms a variable optical phase shift.

The fluorescent intensity on resonance frequency was monitored by a digital oscilloscope as a function of time scanning the phase shifter, as shown in Fig. 4. Each point was measured at an integration time of 5 ms. The interference fringes are well described by a sinusoidal function of the optical phase shift, as expected. The visibility of interference fringes is 0.2 and the signal-to-noise ratio of the fringes is about 100 at integration time of only 5 ms. This corresponds to a phase resolution of 30 mrad. The final alignment of laser beams was performed so as to maximize the interference fringes which were monitored on the oscilloscope.

With an optimum alignment, the visibility of interference fringes was examined at $D=4.5$ mm as a function of laser

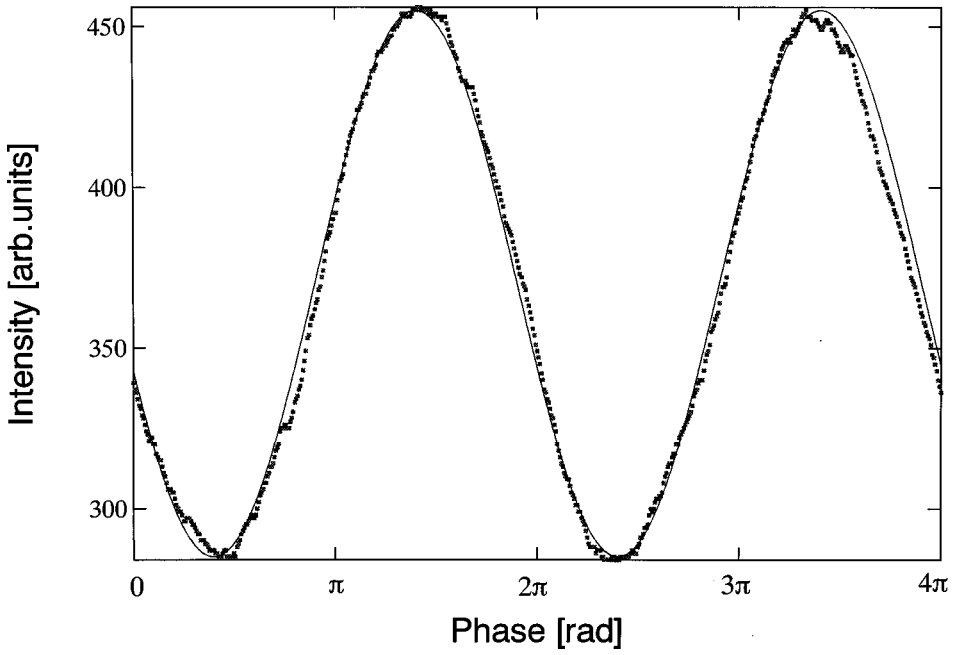

FIG. 4. Interference fringes of atom interferometer as a function of phase, together with a sinusoidal curve (solid line). Data were taken every 5 ms.

power. The results are shown in Fig. 5. The visibility increases as the power increases. The visibility becomes almost maximum at a power of 0.6 mW, which is the pulse area of $\pi/2$ for atoms with the most probable velocity [17]. The visibility of 0.2 could be obtained, but it is smaller than that of 0.5 calculated from Eq. (3) for monovelocity atoms at a pulse area of $\pi/2$.

IV. DISCUSSION

A. Parallelism of laser beams

The visibility of the interference fringes depends strongly on the parallelism of four laser beams. We examined the dependency of the visibility on the parallelism of four laser beams by inclining a pair of laser beams from the other pair by a few milliradian. As shown in Fig. 6, the visibility decreases to half of maximum, when the one pair is deflected by 0.3 mrad from the other. The frequency of the deflected laser beams is shifted by 350 kHz from the resonance frequency due to the Doppler effect. The shift is about twice as large as the transit width [full width at half-maximum (FWHM)] of 180 kHz [18] at the present condition, so that the degree of interference decreases. Therefore, in order to get good interference signals, the parallelism of the four laser beams should be within 0.05 mrad (namely, 10 s or 60 kHz).

If the four laser beams incline from a right angle to the atomic beam by the same inclination, velocity selective interference fringes will be obtained. Although the size of the signal decreases, the visibility increases to a value which is limited by the divergence of the atomic beam.

In the present experiment, each beam waist of the laser beams was located at the interaction zone. For the beam collimation, we used a high-quality 10× microscope lens with a focal distance of 18 mm. When the position of the lens was changed by 0.02 mm, the visibility was reduced to about half of the maximum.

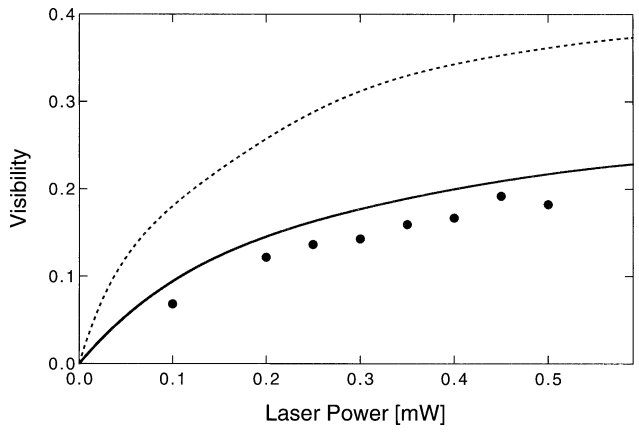

FIG. 5. Visibility versus the excitation laser power, together with the calculated curves. Dotted curve, calculation taking into account the atomic velocity distribution; and solid curve, calculation taking into account the atomic beam divergence in addition.

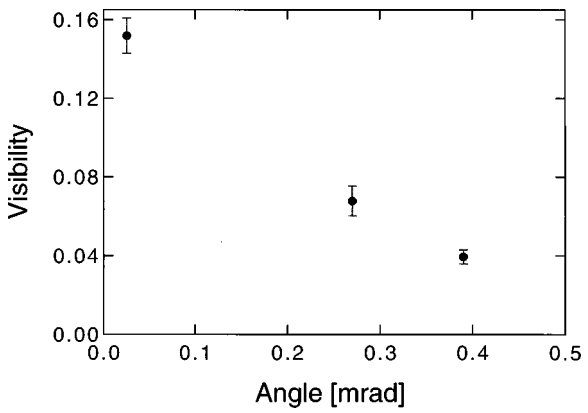

FIG. 6. Visibility versus deflection angle of one pair of laser beams from the other pair of beams.

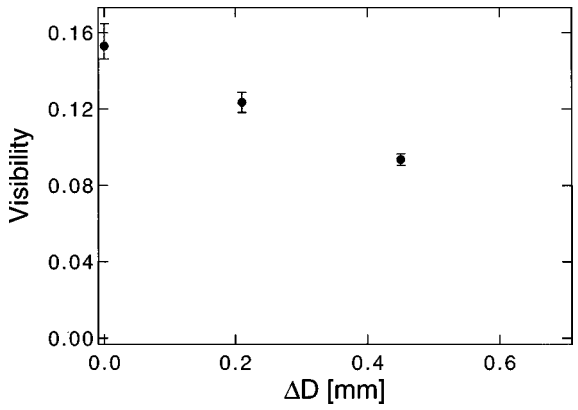

FIG. 7. Visibility versus difference between lengths of two free zones.

B. Difference between beam intervals

The behavior of the visibility was examined when the beam interval between the first and the second beams differs from that between the third and fourth beams. We introduced a thick optical plate into the fourth beam and changed the beam interval between the third and the fourth beams by tilting the thick plate. The visibility was measured as a function of the difference ΔD between two intervals, as shown in Fig. 7. The result shows that the visibility was reduced to half of the maximum at the displacement of 0.5 mm.

In Sec. II we assumed that the beam interval between the first and the second laser beams is the same as that between the third and the fourth. However, if there is some difference ΔD, the phase in the interference terms is given by

$$\varphi=(\Delta-kv_z-\delta)\,\frac{\Delta D}{v_x}+\Delta\phi. \tag{4}$$

The first term is the residual Ramsey fringes which arise as a function of the laser frequency and the third term is a small phase shift due to the atomic path difference. On the other hand, the second term fluctuates depending on v_z times ΔD and finally the fringes disappear as ΔD increases. If we calculate the phase shift for atoms with a most probable velocity, the difference should be 0.5 mm in order to change the phase by 2π rad. The estimation confirms the experimental result. Therefore the difference between two zones should be less than 0.1 mm to get the maximum visibility, although the beam radius is 1.55 mm.

C. Calculation of the visibility

In order to calculate the visibility of the interference fringes, we must take account of the specific features of the Ca atomic beam device; the divergent thermal atomic beam and the interaction physics. The 0.4 ms lifetime of the excited $^3P_1$ state is much longer than the interaction time and the effect of collisions in the atomic beam can be completely neglected. For atoms with the most probable velocity, the transit linewidth is about 180 kHz [18]. The recoil shift of 12 kHz can be neglected. Therefore the nutation frequency Ω, which determines the matrices of A, B, C, and D [15], is given by

$$\Omega=\sqrt{(\omega-\omega_0)^2+\Omega_{ab}^2}. \tag{5}$$

First we consider the thermal atomic beam which interacts with the laser beam perpendicularly. On resonance frequency ω_0, the pulse area depends on the velocity of the atom. When the laser beam is assumed to be a Gaussian beam, for the various velocities of atoms the pulse area in Eq. (3) is given by

$$\theta=\frac{2\mu}{hv_x}\left(\frac{p}{\epsilon_0 c}\right)^{1/2}, \tag{6}$$

where p is the power of each laser beam and μ is the dipole moment. In order to calculate the fluorescence signal detected by a photomultiplier, the Maxwell velocity distribution for the atomic beam at an oven temperature of T, and the position L and diameter l of the photomultiplier were taken into consideration. The equation for the fluorescence signal $bb^*(\omega_0)$ is

$$bb^*(\omega_0)=2\left(\frac{m}{2k_BT}\right)^2\int_0^\infty bb^*(\omega_0,v_x)v_x^3\exp\left(-\frac{mv_x^2}{2k_BT}\right)\times\exp\left(-\frac{\gamma_b L}{v_x}\right)\left\{1-\exp\left(-\frac{\gamma_b l}{v_x}\right)\right\}dv_x, \tag{7}$$

where m is the mass of the Ca atom and k_B is Boltzmann's constant. Using this equation, we calculated the visibility which is given by a dotted line in Fig. 5.

Next, we should take into account the divergence of the atomic beam, which is collimated with two diaphragms. A particular atomic beam diverges with an angle of α from the central atomic beam which interacts with the laser beam normally. The declined beam with α is resonant with the laser beam whose frequency is shifted from ω_0 by $\Delta=\omega_0\alpha v_x/c$ due to the Doppler effect. The profile of beam divergence can be expressed as a function of detuning frequency Δ; $g(\Delta)$. Therefore the declined beam is excited by laser beams with off-resonance frequency. At off-resonance condition, the pulse area depends on the detuning laser frequency as well as the laser power, as shown in Eq. (5). Then the fluorescence signal $I(\omega)$ from the excited state is given by a convolution of functions of $bb^*(\omega)$ and $g(\Delta)$,

$$I(\omega)=\int g(\Delta)bb^*(\omega-\omega_0-\Delta)d\Delta. \tag{8}$$

In the present case, the Doppler linewidth is about one order larger than the transit linewidth. The beam divergence function is assumed to be a Gaussian function with a FWHM of 3.2 MHz. Then the calculated spectra for $p=0.3$ mW are shown in Fig. 8, together with the experimental result, where the calculated peak intensity of the spectrum for $\Delta\phi=\pi$ is normalized to the experimental value. The experimental profiles are reproduced by the calculated profile, although the former is wider at near resonance and narrower far from resonance than the latter. The peak intensity of the calculated spectrum for $\Delta\phi=0$ is a little smaller than the experimental value. A rectangular function and a triangular function as $g(\Delta)$ were also assumed, but there were no significant differences on the peak intensity for $\Delta\phi=0$. Therefore we

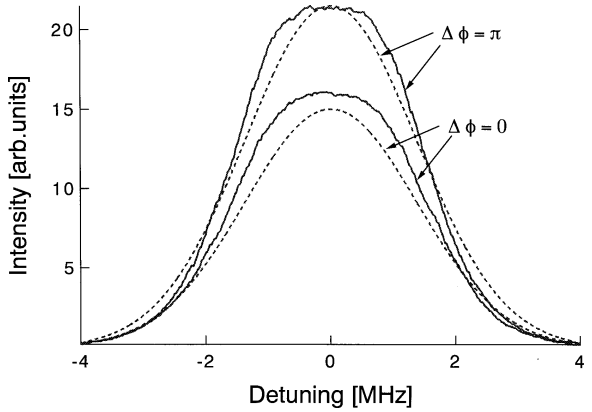

FIG. 8. Experimental (solid curve) and calculated (dashed curve) fluorescence spectra from the excited state with optical phase shift of π and 0 rad. The calculated curve for the optical phase of π rad is normalized to the experimental one.

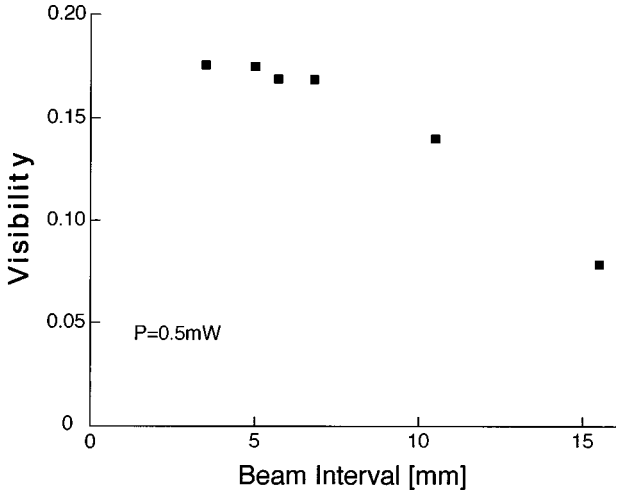

FIG. 9. Visibility versus the beam interval of free zone.

adopted the Gaussian function for the calculation. Thus we calculated the visibility for various laser powers. The calculated results are shown by a solid line in Fig. 5, together with the experimental ones. The experimental results are well described by the calculated curve, although the agreement between the experiment and the calculation is not perfect. We believe a small discrepancy is caused by the intensity distribution of the laser beam in the y direction [19] and the difficulty of achieving perfect alignment in the experiment.

D. Beam interval

The visibility was measured as a function of the beam interval D, as shown in Fig. 9. The visibility at $D=15$ mm decreases to half of that at $D=5$ mm. We can understand from Eq. (3) that the fluorescence signal decreases due to the relaxation as D increases, but the decrease of the visibility is very small. There will be other effects which prevent the interference of atomic waves, in addition to the longitudinal relaxation effect, for example, a transverse relaxation effect of a metastable atom, or phase change of laser beam during the time when atoms travel between the beam interval. From the experimental results, we could expect a visibility of 0.075 with a signal-to-noise ratio of 500 at an integration time of 1 s when the beam interval is 15 mm.

V. CONCLUSION

We investigated the performance of the interference fringes of the atom interferometer comprised of four copropagating laser beams. With a careful alignment, the visibility of interference fringes for a thermal atomic beam was about 0.2 at an excitation power of 0.6 mW and a relatively small beam interval of 5 mm. The signal-to-noise ratio of the fringe was about 100 for an integration time of 5 ms. The experimental results were reproduced well by the calculation using the equation derived for the divergent thermal atomic beam.

As well as the pulsed geometry reported by Kasevich and Chu [4], an interferometer geometry with three beams of $\pi/2$-π-$\pi/2$ sequence separated in space is attractive because it is a simple geometry and expected to get a higher visibility. Recently, we have developed this interferometer and could improve the visibility to 0.3. We plan to publish the details in the future. However, we aim to use the interferometer comprised of four laser beams to measure the Aharonov-Casher effect [10], where the central free zone is important for the measurement.

ACKNOWLEDGMENTS

This experiment was done at the National Research Laboratory of Metrology (Japan) with the kind support of Dr. N. Ito. We thank Y. Ohuchi for his assistance in the preliminary calculation. This work was supported in part by a Grant-in-Aid for Scientific Research (B) of the Ministry of Education, Science and Culture (Japan).

[1] O. Carnal and J. Mlynek, Phys. Rev. Lett. **66**, 2689 (1991).
[2] D. W. Keith, Ch. R. Ekstrom, Qu. A. Turchette, and D. E. Pritchard, Phys. Rev. Lett. **66**, 2693 (1991).
[3] F. Riehle, Th. Kisters, A. Witte, J. Helmcke, and Ch. J. Bordé, Phys. Rev. Lett. **67**, 177 (1991).
[4] M. Kasevich and S. Chu, Phys. Rev. Lett. **67**, 181 (1991).
[5] F. Shimizu, K. Shimizu, and H. Takuma, Phys. Rev. A **46**, R17 (1992).
[6] Ch. J. Bordé, Phys. Lett. A **140**, 10 (1989).
[7] K. Sengstock, U. Sterr, D. Bettermann, J. H. Muller, V. Rieger, and W. Ertmer, in *Fundamentals of Quantum Optics III*, edited by F. Ehlotzky (Springer-Verlag, Berlin, 1993), p. 36.
[8] F. Riehle, A. Witte, Th. Kister, and J. Helmcke, Appl. Phys. B: Photophys. Laser Chem. **54**, 333 (1992).
[9] A. Morinaga, T. Tako, and N. Ito, Phys. Rev. A **48**, 1364 (1993).
[10] K. Zeiske, G. Zinner, F. Riehle, and J. Helmcke, Appl. Phys. B: Lasers Opt. **60**, 205 (1995).
[11] Ch. J. Bordé, in *Laser Spectroscopy*, edited by M. Ducloy *et al.* (World Scientific, Singapore, 1992), p. 239.
[12] M. Kasevich and S. Chu, Appl. Phys. B: Photophys. Laser Chem. **54**, 321 (1992).
[13] A. Morinaga and Y. Ohuchi, Phys. Rev. A **51**, R1746 (1995).

[14] A. Morinaga, M. Nakamura, T. Kurosu, and N. Ito, Phys. Rev. A **54**, R21 (1996).
[15] Ch. J. Bordé, Ch. Salomon, S. Avrillier, A. van Lerberghe, Ch. Breant, D. Bassi, and G. Scoles, Phys. Rev. A **30**, 1836 (1984).
[16] A. Morinaga, N. Ito, and K. Sugiyama, Jpn. J. Appl. Phys., Part 2 **29**, L1727 (1990).
[17] F. Riehle, A. Morinaga, J. Ishikawa, T. Kurosu, and N. Ito, Jpn. J. Appl. Phys., Part 2 **31**, L1542 (1992).
[18] K. Shimoda, in *High-Resolution Laser Spectroscopy*, edited by K. Shimoda (Springer, Heidelberg, 1976), p. 14.
[19] A. Morinaga, Y. Ohuchi, S. Yanagimachi, and T. Tako, in *Proceedings of the Fifth Symposium on Frequency Standards and Metrology*, edited by J. C. Bergquist (World Scientific, Singapore, 1996), p. 243.